Accepted for publication in:

COUPLING BETWEEN THE CALIFORNIA CURRENT SYSTEM AND A COASTAL PLAIN ESTUARY IN LOW RIVERFLOW CONDITIONS

Coupling between the California Current System and a Coastal Plain Estuary in Low Riverflow Conditions

B.M. Hickey, X. Zhang and N. Banas

School of Oceanography, Box 355351
University of Washington, Seattle, WA 98195

Abstract

Willapa Bay, a partially mixed coastal plain estuary, is located on the shoreward side of a narrow, deep continental shelf whose water properties fluctuate on several day scales in response to alternating periods of upwelling and downwelling. Hydrographic surveys as well as water property and velocity time series at a number of sites both within the estuary and on the adjacent coast are used to examine water property and circulation patterns in the estuary during a low runoff period. The data demonstrate that variability is significant (up to 3 psu, ~2 ^{o}C and 10 cm s^{-1} at 5 km from the estuary mouth) and that this variability is determined primarily by the variability in the coastal ocean rather than by estuarine processes such as changes in riverflow or neap-spring variation in mixing. Density changes near the mouth of the estuary that result from upwelling or downwelling of coastal water are consistent with transmission to the estuary primarily through a gravity current mechanism, which modifies the along-estuary density gradient and hence the gravitational circulation within the estuary. Tidal stirring is likely also important to the modification of estuary water properties. New water moves up the estuary at a rate on the order of 10 cm s^{-1}. Associated Eulerian residual velocity fluctuations propagate up estuary about 50% faster than water properties, indicating that up-estuary transmission of the ocean water perturbation may also have internal wave-like characteristics. The modulations in estuarine circulation and water properties lag local wind stress fluctuations (hence, upwelling or downwelling) by more than a day near the estuary mouth and several days farther up the estuary.

1. Introduction

In the majority of estuaries, water property variations on several day and longer timescales are dominated by changes in riverflow into the estuary at its head and/or by processes such as vertical mixing and tidal stirring (e.g., Pritchard, 1956; Geyer and Signell, 1992). Fluctuations in salinity and stratification frequently have a significant relationship to tidal variability; for example, they may demonstrate a strong neap-spring cycle (e.g., Hass, 1977; Sharples et al., 1994). Although not as ubiquitous, contributions to variability originating from the mouth of the estuary have also been observed. For example, salinity variations in Chesapeake Bay have been related to ocean-estuary exchange driven by remote (i.e., shelf) wind stress forcing (Wang, 1979). Similar variability has been related to the presence of a river plume on the shelf at the estuary mouth. Wiseman et al. (1990) showed that water from the Mississippi plume sometimes enters small local estuaries, and water from the Delaware plume has been observed downstream in small embayments (Wong and Lu, 1994). Such intrusions occur during downwelling events when lighter coastal water is pushed toward the coast by surface Ekman currents. Intrusions of denser coastal water into estuaries during coastal upwelling events have also been reported. Off South Africa, Monteiro and Largier (1999) show that dense near bottom water intrusions originating from coastal upwelling control the 6-8 d scale water property variability in a small coastal embayment. In the California Current System, recently upwelled water was observed on the bar at the entrance to San Francisco Bay (Largier, 1996). Nutrient input from an upwelling event was identified in an Oregon estuary (de-Angelis and Gordon, 1985) and seasonal upwelling has been shown to enhance flushing of Grays Harbor, an estuary on the Washington coast (Duxbury, 1979). Dense water intrusions are generally attributed to the baroclinic onshore directed pressure gradient caused by the difference in density between coastal and estuary water (Monteiro and Largier, 1999).

In the California Current System in summer, the relatively narrow and deep continental shelf and the rapidly varying coastal wind field combined with low riverflow into coastal estuaries produce conditions which might be favorable to property control by the ocean rather than the river end of the estuary. In this paper we show that this is indeed the case--using data from Willapa Bay, a coastal plain estuary on the Washington coast, we will demonstrate that during the summertime upwelling-dominant period, estuary water properties have significant water property variability on scales of 3-10 d and that the origin of these variations is almost completely controlled by the oceanic intrusions. Because of its location just north of the Columbia River, the estuary studied has both river plume and

upwelling influences. The comprehensive dataset is unique in that it has sufficient spatial resolution to trace water property changes from the coast up the estuary, to estimate the rate of progression as well as the modifying effect of the intrusion on along-estuary density gradients and estuarine residual velocities, and to determine the dominant mechanisms for the up-estuary advance of the coastal water. Results from this study are likely applicable to many small estuaries located in strongly upwelling regions.

The oceanographic setting for Willapa Bay is described below followed by data and analysis techniques in Section 3. Variability of water properties and Eulerian currents are described in Sections 4 and 5, respectively. In Section 6 results are synthesized to specifically examine the hypothesis that water property and current variability in this coastal plain estuary in the summertime, low runoff period are controlled by variability in coastal upwelling/downwelling on the shelf adjacent to the estuary.

2. Setting

Willapa Bay is one of two large estuaries on the Washington coast (Fig. 1). Willapa is pristine in comparison with many other estuaries, with no overall pollution or impacts from excess nutrient loading. This situation is likely due in part to the flushing processes addressed in this paper. In spite of the fact that Willapa is home to substantial commercial oyster production and provides many recreational opportunities, processes controlling water properties in Willapa have not previously been studied. Willapa is a partially mixed coastal plain estuary with extensive tidal flats divided by deeper channels. The estuary has two branches, one extending east-west for about 19 km (fed primarily by the Willapa and North Rivers) and the other extending north-south for about 29 km (fed by the Naselle River). A second branch at the south end of the estuary (the Nahcotta Channel) has essentially no river input. Although total discharge into the bay can reach 500-1000 $m^3\ s^{-1}$ during a large winter storm, in summer (the period described here) mean discharge is about 15-30 $m^3\ s^{-1}$.

Willapa Bay is separated from the ocean by Long Beach peninsula, a low, sandy spit (Fig. 1). The coastal entrance to the bay is about 10 km wide, with much of the entrance being shoals less than 5 m deep. Most of the water volume flows through two channels in the upper half of the entrance--one, on the north side, a relatively deep (20-30 m) channel about 1 km wide; the other, a shallower channel separated from the main channel by shoals and transitory islands. The latter channel is thought to carry much less volume than the north channel. On the other hand, our data will show that this channel may carry water with less diluted coastal properties farther into the bay than the larger and more strongly mixed north channel. Willapa Bay is not dredged at the present time and channel

depth and location can change during a single winter storm. Consequently, where possible, the topography shown in the figures was modified from charted topography using depths measured in our surveys.

The area of Willapa Bay is 347 km^2 at mean higher high water and 158 km^2 at mean lower low water (Andrews, 1965). Intertidal regions occupy 55% of the area of the Bay, and the ratio of the tidal prism to fluvial discharge is on the order of 200, much larger than for other estuaries in the California Current System (Peterson et al., 1984). The tides are mixed diurnal and semi-diurnal with a diurnal to semi-diurnal amplitude ratio of about 0.55 (Callaway, 1971). The tidal range is 4-5 m, the tidal excursion is about 10 km and the average tidal current amplitude at the entrance to the Bay is about 1.3 m s^{-1} (Andrews, 1965).

Water properties of the Washington shelf in summer are dominated by seasonal upwelling, which brings colder, saltier, nutrient-rich water upward in the water column near the coast (Landry et al., 1989). The variability of water properties on shorter-than-seasonal time scales over the inner shelf is dominated by wind-driven upwelling and downwelling, changing from one to the other on time scales of 3-10 d (Hickey, 1989; Hermann et al., 1989). The buoyant plume from the Columbia River estuary about 40 km south of Willapa Bay (see Figure 1) also plays an important role in water properties of the Washington shelf (Hickey, 1989). The exact location of the plume on a given day depends on the ambient currents at that time and the direction of coastal winds at that time (Hickey et al., 1998; Garcia-Berdeal et al., 2002). Most frequently, the plume from the Columbia is located north of the Columbia estuary mouth during periods of downwelling (northward winds) and southwest during periods of upwelling (southward winds). During even modest downwelling events the plume moves shoreward across the shelf where it can contact the mouth of both Willapa and Grays Harbor estuaries. Thus the presence of the plume amplifies the normal tendency in an upwelling region for fresher water to return to the coast during downwelling events.

3. Data Collection and Analysis

Measurements of currents and water properties in Willapa Bay have been carried out from June 1995 through the present. Data have been collected from moored sensor arrays as well as from repeated CTD surveys. This paper primarily discusses results from a comprehensive study that took place during summer 1995.

The locations of moored arrays are shown relative to the local topography in Figure 1. To provide information on shelf processes an array was also deployed on the nearby shelf. To protect the shelf array from fishing activities the array was located about

10 km north of the Willapa entrance between two existing buoys near the entrance to Grays Harbor. Dominant shelf processes such as upwelling and downwelling are large-scale (> 500 km) in the Pacific Northwest in summer (Hickey, 1989; Denbo and Allen, 1987; Halliwell and Allen, 1987) and should be well represented by the mooring data. Although some local buoyancy-driven effects due to the mooring location at the Grays Harbor entrance may occur on tidal scales, buoyant plumes tend to be shallower than the 20 m data used here, particularly during upwelling events (Hickey et al., 1998). Since observations in a similar bottom depth near the Willapa entrance have shown that the primary effect of buoyancy input on alongshore flow is merely a magnitude enhancement rather than a phase alteration, and also because the two estuaries are similarly forced, we expect alongshore differences between mid water column currents on the inner shelf offshore of the two estuaries at subtidal scales to be minimal. Data from this array are therefore used in the analysis to represent the dominant subtidal current fluctuations offshore of Willapa Bay. The shelf array was deployed for a year; the estuary moorings were recovered after only two months due to the onset of intense fishing in the estuary in late summer.

Arrays were of a taut wire configuration, with upper floatation at about 5 m in the estuary and at 20 m on the shelf. Each array was equipped with two current meters. Electromagnetic current meters (InterOcean S4s) were used at sites where surface gravity waves were expected to be most energetic (W1 and W3 at 10 m and W7 at 20 m). The remaining current meters were mechanical (Aanderaas). No wave-induced Savonius rotor bias was detected at stations where S4s and Aanderaas were paired (not shown). With the shallow depths and the necessity of keeping instruments below the depth of ship traffic, sensor depth was generally 8-15 m from the surface at mean lower low water. Hydrographic data show that these sensors were located in the middle to lower half of the water column, i.e., below the depth where density profiles typically have an inflection (see Section 4). Each S4 was equipped with a temperature sensor; Aanderaas were equipped with both temperature and conductivity sensors to provide salinity data.

Additional data during low runoff periods were obtained in the main channel and in the north and middle channels near the Bay mouth (sites D1, D2 and D3 in Figure 1). Data at D1 were obtained by Walter Frick under the auspices of the Environmental Protection Agency. The data at D2 and D3 were collected by Pacific Engineering International as part of a study of erosion in the Bay. Measurements at these sites were made with bottom mounted RDI acoustic doppler profilers. Data at the three sites were available from June 23-August 15, 1995, August 29-September 11, 1996 and August 29-October 5, 1996, respectively. These data were used only to provide additional spatial information on mean Eulerian flow patterns in Willapa Bay.

Data were edited for outliers and filtered to remove diurnal and higher frequency variability (the "residual" data time series) using a ninth-degree Butterworth filter with a 1/40 hr cutoff frequency (Thomson and Chow, 1980). Conductivity records showed a linear decrease due to biofouling after about 30 days of deployment and were truncated accordingly. Unfortunately, no hydrographic data are available for sensor calibration beyond the initial data records. The electromagnetic current meters as well as temperature sensors on all instruments were relatively impervious to fouling and provide longer time series for analyses.

Hydrographic surveys were performed in May-June 1995 using a Sea-Bird 25 CTD. Data were edited and binned to 1 m averages prior to contouring.

Wind data at the Columbia River buoy (B46029) were obtained from the National Data Buoy Center (see location in Figure 1). Because dominant wind fluctuations in this region are large-scale and the estuary is separated from the ocean only by a narrow (1-2 km wide) low lying sand spit, these data should provide a reasonable representation of winds over the estuary as well as on the adjacent shelf. Wind stress was calculated on hourly wind data according to Large and Pond (1981) and then low pass filtered to remove diurnal and higher frequency energy.

The estuary oceanic entrance is denoted the "mouth"; the river end of the estuary is denoted the "head". Flow within the estuary is referred to as "up-estuary" when it is directed away from the ocean and "down-estuary" when it is toward the ocean. Directions on the shelf are referred to as "alongshore" and "cross-shore", positive northward and eastward, respectively. For consistency, directions in the estuary are taken as positive in the down-estuary (frequently northward) direction. "Mean" flow in this paper denotes flow time-averaged over several days to months. Significance levels were obtained using the number of degrees of freedom estimated from the record length divided by the auto-correlation time scale (Davis, 1976) with significance levels taken from Fraser (1958). Unless otherwise noted, all correlations are significant at the 95% level, which varies from about 0.58-0.71 depending on record length and variable involved.

4. Water Properties

In this section the water properties of Willapa Bay are examined for evidence of ocean forcing. A brief description of data from hydrographic surveys is first presented to provide information on vertical and horizontal gradients of water properties, quantities poorly resolved by the moored sensors. As shown with triangles in Figure 2a, most time series were collected in the mid to lower portion of the water column and in the seaward half of the estuary. Following the discussion of the hydrographic section data, amplitudes

and scales of water property variations in data time series are identified. The variability is quantified using lagged correlations to estimate propagation rates and using EOF analysis to obtain spatial patterns. Resulting amplitude time series are used to derive the temporal relationship to coastal forcing. Finally, along-estuary gradients in properties are examined to test the hypothesis that estuary property gradients are modified by the coastal forcing.

4.1 Hydrographic Surveys

Total river discharge into Willapa estuary from the Willapa, North and Naselle Rivers during the measurement period (extrapolating the gauged data based on gauge location and watershed area) was about 30 m^3 s^{-1} in June and 15 m^3 s^{-1} in July, typical summertime low runoff conditions. Contoured salinity (Fig. 2a) and density (Fig. 2c) sections show that the water column in the main channel of Willapa Bay was weakly stratified under these conditions; i.e., Willapa is "partially mixed" during both ebb and flood periods. The range of salinity and sigma-t over the water column at a given location is about 0.5-2 psu or sigma-t units for the examples shown. The salinity range along the estuary, on the other hand, is about 10 psu or sigma-t units. Salinity indicative of purely oceanic water (> 32 psu) was observed during one ebb tide. Both vertical and lateral stratification are generally greater nearer the river mouths; e.g., in the upper region of the Willapa River channel (Figs. 2a and 2c, upper panels) as well as in the main channel toward the Naselle River (Figs. 2a and 2c, lower left panels).

The temperature range along the main channel is as much as 6 ^{o}C, with warmer temperatures farthest from the ocean (Fig. 2b). Temperature contours, although of smaller range than salinity, have similar spatial structures, indicating that water property variability can be described by either temperature or salinity.

The early June surveys were obtained during an upwelling event in coastal waters (see upwelling-favorable winds in lower right panels of Figure 2). Time series discussed in Section 4.2 confirm that colder (~10 ^{o}C), saltier (~32 psu) and denser (24 sigma-t) water appeared at the mouth of the estuary during this event. The strongest upwelling occurred near June 1. Thus, colder, saltier water is observed on the seaward side of the section obtained on June 2 than from the section obtained on June 4 during a weak downwelling event (Figs. 2a and 2b, middle and lower left panels). For comparison, typical nearshore shelf water has temperatures of 8-12 ^{o}C, salinities of 30-33 psu and densities of 24-25 sigma-t in early summer (Landry et al., 1989).

4.2 Spatial and Temporal Structure of Water Property Fluctuations

Time series of both temperature and salinity demonstrate dramatic fluctuations on time scales of several days (Fig. 3). The amplitude of the fluctuations in both properties is greatest near the estuary mouth (W1) (~3 psu, ~2 ^{o}C). However, significant fluctuations

are also observed at sites halfway along the main channel (W5) (~1.5 psu, ~1 ^{o}C). Salinity near the estuary mouth ranges from about 25 psu to 32 psu during the measurement period. Salinity at the site halfway down the main channel (W5) ranges between about 25 and 30 psu. Comparison with the vertical structure of the hydrographic sections (Figs. 2a,b,c) demonstrates that the property fluctuations cannot be due simply to vertical movement of isopleths--they must represent a horizontal exchange of mass in the estuary.

Temperature at all sites is dominated by seasonal atmospheric heating, increasing almost 6 ^{o}C over the two months shown (Fig. 3). Temperature increases from about 12 to 18 ^{o}C near the mouth and about 14 to 20 ^{o}C halfway down the main channel. At the one site where two depths are shown (W5), temperature is about 0.5 ^{o}C warmer at 10 m than at 15 m, consistent with the vertical gradient observed in the early June hydrographic sections (Fig. 2b).

Water property fluctuations are similar from site to site. The similarity is more apparent in salinity than in temperature because the seasonal trend requires a large scale range, masking the fluctuations. An up-estuary delay in both temperature and salinity signals is also apparent in both figures. It is noteworthy that the delay occurs whether the signal is positive or negative; i.e., for both relatively fresher and relatively saltier pulses. Lagged correlation analysis (in which the time lag for maximum correlation with data at W1 was calculated) demonstrates that temperature and salinity signals advance up-estuary at a rate of about 10-12 cm s^{-1} as determined from regression (Fig. 3, lower panels). Signals move from the site 5 km from the mouth of the estuary (W1) to mid estuary (W5) in about 1.5 d. If this rate of progression were to continue farther up the estuary it would take about 4.5 d for the signal to reach the Naselle River at the southern head of the estuary.

To investigate the spatial structure of water property fluctuations more rigorously, Empirical Orthogonal EigenFunction (EOF) analysis in the time domain was performed on both temperature and salinity time series. To remove ambiguities that might be caused by the signal propagation, the analysis was performed on data lagged to remove propagation with respect to the site near the estuary mouth (W1) (denoted "adjusted" EOFs). For temperature, EOFs were performed both with and without the seasonal trend. Salinity and temperature EOFs were calculated for the periods June 4-July 11 and June 5-July 27, respectively.

For salinity, 91% of the variance is contained in the first mode (Fig. 4a). The amplitude time series for the mode is significantly correlated at the 95% level with alongshore wind ($r = -0.75$) with southward wind (upwelling-favorable) associated with high salinity and northward wind (downwelling-favorable) associated with low salinity. The lag between southward wind and the appearance of colder water at the site closest to

the estuary mouth is 1.5 d. These relationships are consistent with infusion of saltier water into the estuary during periods of coastal upwelling, when deep, cold, salty water is moved onshore and upward close to the coast, and infusion of fresher water (but saltier than estuary water) during coastal downwelling when warmer, fresher surface water is moved onshore. Note that the offshore source of distinctly fresher water in this region is often the Columbia plume. The up-estuary decrease in amplitude of this estuary-ocean coupling is captured by the salinity EOF--amplitude decreases by more than a factor of two between the estuary entrance and the station halfway down the main channel (a distance of about 12 km). Fluctuations are greater in the south channel entrance than in the north channel entrance. At the one location where data are available at more than one depth, the EOF is consistent with an increase in amplitude with depth.

EOF analysis of temperature time series with the seasonal trend included separates fluctuations into two modes, one dominated by seasonal heating (Fig. 4b, left panel); the other dominated by wind-related fluctuations (not shown). The heating mode (87% of the variance) has relatively uniform amplitudes within the bay, consistent with a rise in temperature of about 6 ^{o}C over the two months shown. Amplitudes are slightly greater at shallower depths at every site, consistent with surface heating.

The first temperature EOF mode also contains some wind-related variability in addition to seasonal heating (upper of two time series in Figure 4b). These fluctuations are better resolved using detrended, lag-adjusted data. The first mode of the detrended and lag adjusted EOF captures most of the event scale variance (85%) and the amplitude time series for this mode is weakly correlated with alongshore wind ($r = 0.40$, significant at the 75% level, at a lag of 1.25 d) (Fig. 4b). Colder temperatures are associated with upwelling-favorable wind events and warmer temperatures with downwelling-favorable wind events. The lag between southward wind and the appearance of colder water at the site closest to the estuary mouth is 1.25 d. The spatial structure of the lag-adjusted, detrended EOF suggests an up-estuary amplitude decay of more than a factor of two over about 12 km (Fig. 4b, right panel). In contrast to the heating mode, amplitudes generally increase toward the bottom (as for the salinity EOF).

Along-estuary gradients in temperature, salinity and density also demonstrate significant fluctuations on several day time scales (Fig. 5). Both salinity and density gradients are reversed during some downwelling events. Although such reversals might be due to intrusions of fresher-than-estuary water associated with the plume from the Columbia River, as has been observed in more recent datasets, the reversals may also be due to undetected biofouling of the conductivity sensors. This conclusion is based on the fact that no differences were seen during the events with such "reversals"--up-estuary

propagation still occurred, for example (Fig. 3), suggesting that the dynamics have not changed dramatically as might be expected if the longitudinal density gradient in the estuary had changed sign. Fluctuations in along-estuary density differences (which do not depend on the potentially biased means) demonstrate a strong relationship to salinity--with larger gradients when salinity near the mouth is higher ($r = 0.83$; Fig. 5, middle right panel). This shows that along-estuary density gradients are greater following coastal upwelling events than following coastal downwelling events. Note also that up-estuary propagation speed was generally faster during upwelling than during downwelling events--e.g., between W1 and W5, the average speed of salinity signal propagation was 36.5 and 13.8 cm s^{-1} during 5 upwelling/4 downwelling events, respectively. Similar results were obtained between other pairs of stations.

In summary, water property data have shown, for the first time, detailed characteristics of ocean-forced water property fluctuations in a coastal plain estuary in the California Current System; namely, a lagged relationship to alongshore (or estuary) wind, a tendency for signals to propagate up the estuary, with faster propagation during upwelling events, and a tendency for along-estuary property gradients to be related to the salinity at the estuary mouth. Amplitudes of fluctuations decrease up the estuary and toward the surface. In the following section, similar (and related) fluctuations are shown to exist in the Eulerian residual velocity field.

5. Eulerian Residual Currents

In this section, the Eulerian velocity field of Willapa estuary is examined for evidence of ocean forcing. The mean is first presented to provide a context for the more detailed analysis of velocity fluctuations. Next, spatial and temporal patterns are determined using lagged correlations and EOF analysis. Temporal variations of the EOF amplitude time series are used to test for a relationship with the coastal forcing. Finally, velocity fluctuations are related to the water property fluctuations discussed in the preceding section.

Time series of vector velocities at selected sites display significant means as well as significant fluctuations about the means and both have similar magnitudes (~5-10 cm s^{-1}) (Fig. 6). At the shelf site (W7), as expected from past research, much of the variability is clearly related to alongshore wind ($r = 0.73$), with current lagging wind by 0.5 d, typical for wind-driven alongshore currents on the inner shelf (Hickey, 1989). These results are consistent with the assumption that residual currents at the W7 site are representative of relatively large scale wind forcing during this period. Typical velocity amplitudes within the estuary are roughly half those on the adjacent shelf.

5.1 Eulerian Mean Circulation Patterns

To provide quantitative information on spatial structure of the mean flow field, velocity data were averaged over available record lengths from summer 1995. Means for sites D1, D2 and D3, all obtained in low riverflow conditions, were also calculated over their complete record lengths. We note that vector time series for the summer 1995 period indicate that mean flow patterns over at least this period are relatively robust (Fig. 6).

Mean speeds ranged from about 2 cm s^{-1} in the Nahcotta Channel to 20 cm s^{-1} in the main north-south channel as well as the channels near the estuary mouth (Fig. 7). The direction of the mean flow is strongly modified by local bathymetry. For example, currents are directed northwest in the north entrance channel, but southwest in the south entrance channel. Currents at W2 are directed due north rather than along the east-west channel at this site. It seems likely that the measurement site is in a small eddy (perhaps a tidal residual flow) related to the channel entrance near Toke Point. The strongest down-estuary currents are clearly in the main channel near the estuary mouth. However, the strongest up-estuary currents are observed at W4 in the central estuary. Note that mean currents at that site oppose those at similar depths at the site just 6.5 km south (W5).

The measurement grid is insufficient to describe the complete vertical and lateral flow structure--instruments are generally in the middle or lower water column and at only one location on any cross-estuary section. Even at sites with data spanning most of the water column (D1, D2, D3), the mean flow is uni-directional at a single site. However, stronger up-estuary flow or weaker down-estuary flow is observed at deeper depths. Mean down-estuary flow occurs at sites near the mouth and in the central deep channel (W5). Mean up-estuary flow occurs at the other sites. As will be shown later, the pattern of velocity fluctuations has the same sign as that of the mean flow--i.e., if the mean flow is oppositely directed at two sites, so are the fluctuations. We note that the sites where the mean flow is up the estuary (W4, W6 and D1) are all located in the vicinity of extensive intertidal banks.

Lateral variation in estuarine residual flows is frequently observed (e.g., Jay and Smith, 1990, for the Columbia estuary; Wong, 1994 for Delaware Bay; and Kjerve, 1986 for North Inlet, North Carolina). Li et al. (1998) provide an excellent review of residual circulation resulting from both the gravitational circulation and tidally induced flows in estuaries with laterally varying cross-sections. For a gravitational circulation pattern in rectangular channel topography (e.g., Pritchard, 1956; Hansen and Rattray, 1965) we expect up-estuary flow in the lower water column and down-estuary flow in the upper water column; in an estuary with laterally-varying topography, on the other hand, we might expect the mean gravitational flow to be predominantly up-estuary in the channels and down-estuary over shallower regions (e.g., Fischer, 1972; Wong, 1994). The tidally-

induced circulation, primarily a response to inward Stokes drift (Ianniello, 1977), has an opposite pattern to the gravitational circulation in laterally varying topography (Li and O'Donnell, 1997). Thus, the gravitational and tidally-induced circulations compete, with the competition in the vertical plane for rectangular cross-sections and in the lateral direction for non rectangular cross-sections. In addition we note that an estuary with complex three dimensional topography like Willapa is likely to have substantial rectification near local topographic features (Signell and Geyer, 1990). Wind forcing over the estuary might also cause mean circulation patterns (Wang, 1979). However, the site to site difference in along-channel mean flows observed in Willapa suggests that this is not likely the dominant mechanism responsible for the observed mean flow patterns. With this background, we conclude that the dominant mean flow pattern is suggestive of tidally-induced mean residual flows rather than gravitational circulation--down-estuary in the channels and up-estuary in shallower regions. We note that the presence of significant Stokes drift might result in particle and mass transports that deviate significantly from Eulerian transports (Geyer and Signell, 1990; Kuo et al., 1990). The mean vertical shear consistent with greater up-estuary flow at depth may be the signature of a weak gravitational circulation.

5.2 Spatial and Temporal Structure of Velocity Fluctuations

Time series of de-meaned dominant flow components (either u or v, whichever is more closely parallel to the direction of local topography) show that shelf and estuary currents appear to be correlated at sites nearest the estuary mouth ($r = 0.50$, significant at the 90% level) (Fig. 8). In addition we note that velocity time series exhibit much more spatial variability than corresponding time series of temperature and salinity (compare Figures 3 and 8). Nevertheless, as for salinity and temperature data, lagged correlation analysis demonstrates up-estuary velocity signal propagation, with a lag of about 0.8 d over 12 km from near the mouth to the middle of the estuary (W1 to W5) and a delay with respect to the wind of 1.25 d near the estuary mouth (W1) and up to 1.75 d at the mid estuary site (W5) (Fig. 8, lower panels). Note that the same propagation rate was observed from the shelf to the estuary as up the estuary. For this calculation the shelf fluctuations were assumed to occur just offshore of Willapa Bay, as justified in Section 3. Note that propagation rate for the velocity signal is about 30% greater than for temperature and salinity (16 vs. 10-12 cm s^{-1}). At most sites southward flow on the shelf and southward wind on the shelf (or in the estuary) are associated with up-estuary flow.

EOF analysis of the lag-adjusted velocity field for the period June 8-July 2 demonstrates that 74% of the variance is contained in a mode which describes a coherent spatial pattern of down-estuary flow at most sites and northward flow along the shelf (or the reverse pattern) (Fig. 9, upper panel). As for salinity and temperature, fluctuations are

stronger in the south entrance channel (W1) than in the north channel (W3). The amplitude time series for this mode is strongly coherent with alongshore wind (r = 0.85 with a 1.0 d lag; Fig. 9, lower panel). Thus, with the exception of sites where mean flow was up-estuary (W4 and W6), when wind and shelf currents are southward over the shelf (upwelling-favorable), up-estuary flow is enhanced; when wind and currents are northward (downwelling-favorable) over the shelf, up-estuary flow is retarded.

In addition to the relationship with alongshore wind, along-estuary velocity fluctuations show a significant relationship to both near mouth salinity and along-estuary density differences--the greater the salinity near the mouth or the along-estuary density difference the greater the up-estuary flow tendency (the weaker the down-estuary flow) (Fig. 5). The correlation with along-estuary density difference is - 0.72 near the estuary mouth and - 0.61 at mid estuary.

EOF analysis indicates greater velocity amplitudes at deeper depths at the site near the estuary mouth as observed for both temperature and salinity fluctuations (Fig. 9). Data at two depths are also available at sites W4 and W5 although for shorter time periods than used in the EOF analysis. At both sites, regression analysis also shows greater velocity amplitudes closer to the bottom. Amplification factors over 5 m (~20% of the water column) were 1.2 (r = 0.92) and 1.1 (r = 0.64) at W4 and W5, respectively.

6. Discussion

The data demonstrate that large amplitude low frequency (< 1 cpd) fluctuations occur in both water properties and currents of Willapa estuary. The fact that the amplitude of the fluctuations decreases away from the estuary mouth and that the fluctuations are related to the coastal wind field (with denser, colder and saltier water following periods of southward winds) demonstrates a relationship to coastal upwelling over the adjacent shelf. Thus the data demonstrate that the primary modification of estuarine water properties is a result of coastal upwelling and downwelling rather than changes in river influx or tidal mixing characteristics.

The observed timing and spatial structure of the fluctuations (summarized in Figure 10) also suggests a mechanism by which new coastal water propagates up the estuary. Water property fluctuations near the estuary mouth lag the alongshore wind by about 1.5 d (r = - 0.64, significant at the 95% level). Propagation up the estuary occurs at a rate on the order of 10 cm s^{-1}, usually with faster propagation following upwelling events. Fluctuation amplitudes increase toward the bottom for both water properties and velocity. The fluctuations modify the along-estuary density gradients and also the along-estuary velocity field. Finally, the magnitude of the fluctuations is much larger than can be accounted for by

vertical movement of mass, indicating that horizontal exchange of mass must occur. These characteristics are broadly consistent with a mechanism involving a gravity current (Benjamin, 1968). A gravity current with a fortnightly modulation was reported in Puget Sound, a deep fjord, propagating away from the entrance sill (Geyer and Cannon, 1982). A later observational study demonstrated that intrusions were a result of fluctuations in the horizontal density gradient over the sill at the entrance to the sound (Cannon et al., 1990). Monteiro and Largier (1999) suggest that the propagation of dense water from the coast into a small coastal embayment in South Africa occurs via a gravity current.

The rapid onset of density changes at the estuary mouth following coastal upwelling (as little as 3 hr; Hickey, 1989) suggest that the dynamics might best be approximated by a lock exchange mechanism (e.g., Simpson, 1987). In this scenario, two adjacent water masses with different densities are released from rest and the denser fluid intrudes beneath the lighter fluid as a gravity current. Unfortunately, the complete estuary setting, including the fact that the receiving fluid is vertically stratified, that it has longitudinal density gradients and that it has ambient currents (in this case opposing the flow, at least in the channels) is poorly understood. Nevertheless, for an order of magnitude estimate of initial propagation speed, following experimental results for a rectangular channel and flows of constant density, the propagation speed is given by

$$c = 0.47 \sqrt{g'H}$$

where g' is reduced gravity, with the density difference given by the difference in density between the two fluids, and H is the channel depth. This is the speed taken by the gravity current on initiation of lock exchange. Speed decreases at later times in the loch exchange problem as other dynamics dominate; we note that our observations showed a relatively constant speed throughout the measurement range. If the available density contrast is about 3 sigma-t units for upwelling events (taken from the difference between upwelling and downwelling density in Figure 5) and about 0.5 sigma-t units for downwelling events (taken from the downwelling event on May 28 shown in Figure 2c), then the range of speeds is 36-15 cm s^{-1} following upwelling and downwelling, respectively. This compares favorably with the observed speed difference between the two regimes (a predicted enhancement of 2.4 vs. the observed 2.7 during upwelling events). The existence of ambient flows would be expected to retard the propagation by about 3/5 of the ambient flow speed (Simpson, 1987), in this case about 5 cm s^{-1}.

Up-estuary propagation might also occur via an internal wave mechanism as described in, for example, MacCready (1999), who models the adjustment of estuaries to density perturbations at the estuary head. The complex Willapa situation, in which the density perturbation at the mouth of the estuary encounters pre-existing stratification and

vertical shear as well as along-estuary density gradients, has some similarity to the MacCready study in that freshwater interacts with the pre-existing gravitational circulation and stratification. Moreover, internal waves may be generated by a gravity current intruding into a stratified fluid (e.g., Simpson, 1982, 1987). Laboratory models have demonstrated situations in which both waves and gravity currents are present and the wave can outrun the primary density disturbance (e.g., Figure 5 in Simpson, 1982). The observed ~50 % difference in statistically averaged propagation speeds between velocity and property disturbances, with velocity faster than water properties, suggests that some component of the process may indeed be "wave-like", at least in the sense that the velocity perturbation outruns the water property disturbance. Unfortunately, propagation speeds alone are insufficient to determine whether the likely complex mechanisms involved are better described as a gravity current or as an internal wave (or indeed whether either mechanism is strictly appropriate)--the range of uncertainty in parameter choices produces speed differences greater than the expected differences between the two mechanisms. In particular,, calculation of propagation speeds depends on density contrasts, and, for the internal wave, knowledge of layer depth (if indeed distinct layers exist). Because of the placement of the current meters no time-dependent information is available on these parameters. For an order of magnitude estimate of internal wave speed, if we assume that the estuary has two layers, with an upper layer of depth 5 m (h_1) and a lower layer of depth 15 m (h_2), the resulting speed (Gill, 1982) is given by

$$c = \sqrt{g' \frac{h_1 h_2}{H}}$$

Thus, for a vertical density contrast of 1.5 sigma-t units (see the June 2 upwelling event in Figure 2c) the estimated speed of 23.5 cm s^{-1} falls within the range of estimated speeds we estimated for a gravity current.

Whatever the exact mechanism (s) of up-estuary propagation, the gravitational circulation in Willapa Bay, as indicated by the along-estuary density gradient, is modified each time the coastal density changes. Furthermore, the slope of the density gradient-velocity correlation (shown in Figure 5) is consistent with that predicted by a simple model of density-driven exchange, following Hansen and Rattray (1965). Balancing the baroclinic pressure gradient with vertical diffusion of momentum, we expect exchange-flow velocity to scale with the along-channel density gradient like

$$u_{exch} = \left(\frac{g \quad H^3}{48 \rho_0 K_v} \right) \frac{\partial \rho}{\partial x}$$

where H is the channel depth, ρ_0 is a reference density and K_v is a constant vertical diffusivity. The observed slope between velocity and density gradient corresponds, for a

mean depth of 20 m, to a diffusivity of 60 $cm^2\ s^{-1}$, a typical value for a shallow estuary with strong tidal flow (MacCready, 1999).

An alternate explanation for up-estuary delay of velocity and water property signals is dispersion by nonlinear tidal effects such as topographically driven tidal residuals, Stokes drift, tidal rectification and stirring by transient horizontal eddies. In the simplest formulation, these effects can be modeled as one-dimensional Fickian diffusion, with an effective horizontal diffusivity of K_H. By this mechanism new oceanic water masses will travel up the estuary with lag times (T) that increase quadratically with distance (L) from the mouth according to $L^2 \sim K_H T$, to within a small factor. A detailed examination of the role of tidal stirring is beyond the scope of this paper and is considered in greater detail elsewhere (Banas et al., 2002). Here we note that the curvature of this relationship would be small in the lower estuary where our observations were made. The relationship would be further flattened toward the observed roughly linear relationship if K_H decreases with distance from the mouth as is generally expected (e.g., Hansen and Rattray, 1965). Observed lags are consistent with a diffusivity on the order of 1000 $m^2\ s^{-1}$. Diffusivities on this scale are not uncommon in tidal waters (Zimmerman, 1986) and in fact we might expect even larger values in the seaward reach of a wide, macrotidal estuary like Willapa (MacCready, 1999). Note also that tidal mechanisms for up-estuary salt flux are not necessarily separable from the time-variable gravitational circulation. A tidal residual eddy field may yield chaotic Lagrangian trajectories on its own, but the dispersive effect of horizontal tidal stirring is much amplified by the presence of vertical shear (Zimmerman, 1986). Thus coupling between tidal and density-driven flow might produce the largest up-estuary fluxes (Geyer, pers. comm.).

Our results have shown that wind-related processes dominate the spatially organized variance in estuary velocity and salinity records. To determine whether the neap-spring variation in tidal amplitude accounts for any of the remaining observed variance, the wind-driven variance was removed from original residual time series, using the observed time lag at maximum correlation to ensure maximal removal of the wind-driven variance. A weak relationship between along-estuary velocity and tidal amplitude was indeed observed ($r = 0.55$, ; see Figure 10, bottom panel) although the short record lengths preclude meaningful statistics. Based on the calculated relationship, this effect contributes only 16% to measured velocity fluctuations, roughly one third of the variance accounted for by alongshore wind. The positive correlation between enhanced outflow and tidal height is consistent with a tidally-induced outflow as seen by Kjerfve (1986), rather than with a gravitational flow, which would have the opposite relationship to tidal height (e.g., Linden and Simpson, 1988). No relationship was found between tidal amplitude and salinity,

along-channel gradients in salinity or vertical gradients in salinity (not shown)--maximum correlation coefficients were less than 0.3 in every case.

The focus in this paper has been on exchange and modification of water masses between the coast and the estuary, a process driven by alongshore wind stress over the inner shelf adjacent to the estuary. Our data indicate that the role of alongshore wind stress is to alter (via upwelling or downwelling) the water mass next to the estuary mouth, thereby changing the baroclinic pressure gradient at the estuary mouth. Barotropic low frequency estuary-ocean exchange due to coastal setup by has been reported in a number of estuaries (e.g., Wang and Elliot, 1978; Wang, 1979; Walters, 1982; Walter and Gartner, 1985). However, the response we observed was not vertically uniform, the lag with respect to sea level setup (in phase with alongshore flow) was longer than would be expected (days rather than hours) and the associated velocity fluctuations are in the opposite direction than expected (e.g., enhanced inflow rather than enhanced outflow was observed during periods of lowered sea level such as occurs with equatorward alongshore flow or upwelling events). The relative dominance of baroclinic forcing in Willapa may be due in part to the comparatively large density changes (up to 3-4 sigma-t) presented at the estuary mouth because deep upwelled waters can easily reach the coast within a few hours in this Eastern Boundary System.

It is also worth noting that direct effects of wind stress on the surface of the estuary are not prominent in this data set. For example, no evidence of wind-driven mixing and modification of the estuary density field as reported by Morteiro and Largier (1999) was observed. Wind-forced subtidal scale currents and/or salinity changes have been observed in a number of estuaries. At the extreme of very shallow estuaries (1-2 m depth), currents move downwind at all depths and wind-driven flushing can control the estuary residence time (Geyer, 1997). At the other depth extreme, in Alberni Inlet, a deep fjord, downwind currents were observed only in a shallow surface layer (Farmer and Osborn, 1976) as also observed in the shallower Chesapeake Bay (Wang, 1979). Currents opposing the wind (but strongly correlated to it) were measured in the Providence River in Narragansett Bay, a partially mixed estuary with narrow channels (Weisberg, 1976) and in the Potomac River (Elliott, 1978). Counter-wind flow is produced by the sea surface slope that develops opposing the wind stress (e.g., Wang, 1979). In an estuary with intertidal banks, we might expect downwind flow over the shallow banks, with upwind compensating flow in the deeper channels (Fischer, 1979). Wind-driven currents can exceed the magnitude of the gravitational or tidally-induced residual circulation so that wind stress forcing can enhance or diminish the gravitational or tidally-induced circulation and can even result in three layer residual flow. The Willapa data presented here, however, are not consistent with direct

wind forcing over the estuary as a dominant forcing mechanism for the subtidal flow or salinity fields. First, the lag between wind stress and currents (up to 1.8 d) is much greater than expected for frictional wind driving--about 1.75 d longer than observed by Weisberg (1976) or by Farmer and Osborn (1976)--yet not long enough to be consistent with counterflow due to a sloping sea surface. Second, velocity amplitudes increase toward the bottom rather than toward the surface as would be expected for direct surface forcing. Last, wind crosses the estuary rather than paralleling it along the northern channel where the strongest wind related velocity signals were observed. Statistical comparison of the variance remaining after the remotely driven wind effects, appropriately lagged, were removed produced no significant relationship with wind stress (not shown). It seems likely that the highly three dimensional topography of Willapa estuary produces a complex pattern of directly wind driven flows that are not resolved with the available data set. The relative importance to Willapa Bay of local wind and remote sea level forcing in comparison to the baroclinic forcing described herein is the subject of ongoing research that includes numerical model studies.

7. Conclusions

Measurements in Willapa Bay, a coastal plain estuary located in an Eastern Boundary Current System, show that water property and current variability on scales of several days are determined primarily by offshore variability in coastal upwelling adjacent to the estuary. The modulations in estuarine circulation and water properties lag local alongshore wind stress fluctuations (hence, upwelling or downwelling) by one to several days. Density changes near the mouth of the estuary that result from upwelling or downwelling of coastal water appear to be transmitted up the estuary primarily through a gravity current/internal wave mechanism, modifying the along-estuary density gradients and hence the gravitational circulation as they pass. New coastal water moves up the estuary at a rate on the order of 10 cm s^{-1}. Order of magnitude estimates suggest that tidal stirring likely contributes to the up-estuary and upward water property movement; however, the time-variable magnitudes of these processes could not be determined with the available dataset.

Principal results are summarized in a conceptual model for baroclinic coupling of coastal and estuarine processes in an upwelling dominated, low riverflow setting. In terms of water properties, our conceptual model shows warmer and fresher water offshore (but still colder and saltier than in the estuary) during downwelling periods and colder, saltier water offshore during upwelling periods (Fig. 11). These water masses are advected into the estuary during flood tide and mixed with remaining estuary water. Our results show

that it takes a number of semi diurnal tidal cycles for the coastal water to move into more distant parts of the estuary (about 3 cycles to move 12 km). If we extrapolate the rate of movement obtained in the northern half of the estuary and assume mixing rates are similar over the southern half of the estuary, it would take about 4.5 d for new ocean water to reach the southern head of the estuary.

In general, low frequency fluctuations of currents and water properties within estuaries are complex. In this paper we have focused on the dominant mechanism producing changes in a coastal plain estuary in the California Current System--a baroclinic coupling to coastal upwelling processes during low runoff conditions. Separation of competing mechanisms is difficult because processes such as local wind driving in the estuary and coastal upwelling operate on the same time scale in many small West Coast estuaries, in which the winds over the estuary are virtually identical to the coastal winds. In the present data set, the dominant process was only identified due to its long lag with respect to the local wind. To separate low frequency processes in general, it will be necessary to use a well configured model or to make measurements in sites selected for the expected dominance of a single process. Finally, we note that any model of an estuary such as Willapa must include processes that occur over and near the extensive mud flats, which have been largely ignored in the present paper.

Acknowledgments

Support for measurements obtained in this project was provided to B. Hickey by Washington Sea Grant (grant # NA36RG0071-AM09) as well as the Environmental Protection Agency (contract # DW13717701-M4114). Analysis was supported by Washington Sea Grant (grant # NA76RG0119 and NA76RG0119-AM08) and by the Pacific Northwest Ecosystem Research Study (PNCERS) (grant # NA76RG0485 and NA96OP0238 from the Coastal Ocean program of the National Oceanic and Atmospheric Administration). Data at site D1 were provided by Walter Frick of the EPA. The Doppler current meter data at sites D2 and D3 were provided by Vladmir Shepsis of Pacific International Engineering Co. under a contract from the Washington State Department of Transportation. Dale Ripley was responsible for moored arrays; N. Kachel assisted in CTD processing and data display and S. Geier was responsible for initial data processing and editing. We appreciate the assistance of David Jay's research team as well as the loan of their CTD on the June 1995 cruise. We would particularly like to thank Dennis Tufts and the Bendickson's Oyster Co. for providing ship support for several of the mooring deployments. Conversations with Susan Allen and with Parker MacCready were extremely helpful.

References

Andrews, R.S. 1965. Modern sediments of Willapa Bay, Washington: a coastal plain estuary. Univ. Washington, Dept. Oceanogr. *Tech. Rep. No. 118.*

Banas N.S., B.M. Hickey, J.A. Newton and P.M. MacCready (2002) Tidal-residual and density-driven controls on oceanic exchange in a highly unsteady coastal plain estuary (Willapa Bay). *J. Phys. Oceanogr.* In Prep.

Benjamin, T.B. 1968. Gravity currents and related phenomena. *J. Fluid Mech.* 31: 209-248.

Callaway, R.J. 1971. Applications of some numerical models to Pacific Northwest estuaries. Proceedings, Technical conference on estuaries of the Pacific Northwest, *Sea Grant Circular No. 42*, Oregon State University.

Cannon, G.A., J.R. Holbrook and D.J. Pashinski. 1990. Variations in the onset of bottom-water intrusions over the entrance sill of a fjord. *Estuaries* 13: 31-42.

Davis, R.E. 1976. Predictability of sea surface temperature and sea level pressure anomalies of the North Pacific. *J. Phys. Oceanogr.* 6: 249-266.

de-Angelis, M.A. and L.I. Gordon. 1985. Upwelling and river runoff as sources of dissolved nitrous oxide to the Alsea estuary, Oregon. *Est. Coast. Shelf Sci.* 20 (4): 375-386.

Denbo, D.W. and J.S. Allen. 1987. Large-scale response to atmospheric forcing of shelf currents and coastal sea level off California and Oregon: May-July, 1981 and 1982. *J. Geophys. Res.* 92 (C2): 1757-1782.

Duxbury, A.C. 1979. Upwelling and estuary flushing. *Limnol. Oceanogr.* 24 (4): 627-633.

Elliott, A.J. 1978. Observations of the meteorologically induced circulation in the Potomac estuary. *Est. Coast. Mar. Sci.* 6: 285-300.

Farmer, D.M. and T.R. Osborn. 1976. The influence of wind on the surface of a stratified inlet. Part I. Observations. *J. Phys. Oceanogr.* 6: 931-940.

Fischer, H.B. 1972. Mass transport mechanisms in partially stratified estuaries. *J. Fluid Mech.* 53: 671-687.

Fischer, H. 1979. *Mixing in inland and coastal waters*. Academic Press, New York, 483 pp.

Fraser, D.A.S. 1958. *Statistics: an Introduction*. Wiley and Sons, Inc., New York, 398 pp.

Garcia-Berdeal, I., B.M. Hickey and M. Kawase. 2002. Influence of wind stress and ambient flow on a high discharge river plume. *J. Geophys. Res.* In Press.

Geyer, W.R. 1997. Influence of wind on dynamics and flushing of shallow estuaries. *Est. Coast Shelf Sci.* 44: 713-722.

Geyer, W.R. and G.A. Cannon. 1982. Sill processes related to deep water renewal in a fjord. *J. Geophys. Res.* 97: 7985-7996.

Geyer, W.R. and R.P. Signell. 1992. A reassessment of the role of tidal dispersion in estuaries and bays. *Estuaries* 15: 97-108.

Gill, A.E. 1982. *Atmosphere-Ocean Dynamics*. Academic Press, 662 pp.

Halliwell, Jr., G.H. and J.S. Allen. 1987. Large-scale coastal wind field along the west coast of North America, 1981-1982. *J. Geophys. Res.* 92 (C2): 1861-1884.

Hansen, D.V. and M. Rattray, Jr. 1965. Gravitational circulation in straits and estuaries. *J. Mar. Res.* 23: 104-122.

Hass, L.W. 1977. The effect of spring-neap tidal cycle on the vertical salinity structure of the James, York and Rappahannock rivers, Virginia, U.S.A. *Est. Coast. Mar. Sci.* 5: 485-496.

Hermann, A., B.M. Hickey, M. Landry and D. Winter. 1989. Coastal upwelling dynamics. In: Landry, M.R. and B.M. Hickey (eds.), *Coastal Oceanography of Washington and Oregon*, pp. 211-253, Elsevier Science, Amsterdam, The Netherlands.

Hickey, B.M. 1989. Patterns and processes of circulation over the shelf and slope. In: B.M. Hickey and M.R. Landry (eds.), *Coastal Oceanography of Washington and Oregon*, Landry, pp. 41-115, Elsevier Science, Amsterdam, The Netherlands.

Hickey, B.M., L.J. Pietrafesa, D.A. Jay, and W.C. Boicourt. 1998. The Columbia River plume study: Subtidal variability in the velocity and salinity fields. *J. Geophys. Res.* 103: 10,339-10,368.

Ianniello, J.P. 1977. Tidally induced residual currents in estuaries of constant breadth. *J. Mar. Res.* 35: 755-786.

Jay, D.A. and J.D. Smith. 1990. Circulation, density structure and neap-spring transitions in the Columbia River estuary. *Progr. Oceanogr.* 25: 81-112.

Kjerve, B. 1986. Circulation and salt flux in a well mixed estuary. In: J. van de Kreeke (ed.), *Physics of Shallow Estuaries and Bays*, Vol. 16, pp. 22-29, Springer-Verlag, New York.

Kuo, A.Y., J.M. Hamrick and G.M. Sisson. 1990. Persistence of residual currents in the James River estuary and its implication to mass transport. In: R.T. Cheng (ed.), *Coastal and Estuarine Studies 38: Residual currents and long-term transport*, pp. 389-401, Springer-Verlag, New York.

Landry, M.R., J.R. Postel, W.K. Peterson, and J. Newman. 1989. Broad-scale distributional patterns of hydrographic variables on the Washington/Oregon shelf. In: M.R. Landry and B.M. Hickey (eds.), *Coastal Oceanography of Washington and Oregon*, pp. 1-40, Elsevier Science, Amsterdam, The Netherlands.

Large, W.G. and S. Pond. 1981. Open ocean momentum flux measurements in moderate to strong winds. *J. Phys. Oceanogr.* 11: 324-336.

Largier, J.L. 1996. Hydrodynamic exchange between San Francisco Bay and the ocean: the role of ocean circulation and stratification. In: Hollibaugh (ed.), San *Francisco Bay: The Ecosystem*, pp. 69-105, Amer. Assoc. Adv. Sci.

Li, C., A. Valle-Levinson, K.C. Wong and K.M.M. Lwiza. 1998. Separating baroclinic flow from tidally induced flow in estuaries. *J. Geophys. Res.* 103(C5): 10,405-10,417.

Li, C. and J. O'Donnell. 1997. Tidally induced residual circulation in shallow estuaries with lateral depth variation. *J. Geophys. Res.* 102: 27,915-27,929.

Linden, P.F. and J.E. Simpson. 1986. Gravity-driven flows in a turbulent fluid. *J. Fluid Mech.* 172: 481-497.

Linden, P.F. and J.E. Simpson. 1988. Modulated mixing and frontogenesis in shallow seas and estuaries. *Cont. Shelf. Res.* 8: 1107-1127.

MacCready, P.M. 1999. Estuarine adjustment to changes in river flow and tidal mixing. *J. Phys. Oceanogr.* 29: 708-726.

Monteiro, P.M.S. and J.L. Largier. 1999. Thermal stratification in Saldanha Bay (South Africa) and subtidal, density-driven exchange with the coastal waters of the Benguela Upwelling System. *Est. Coast. Shelf Sci.* 49: 877-890.

Peterson, C., K. Scheidegger, P. Komar, and W. Niem. 1984. Sediment composition and hydrography in six high-gradient estuaries of the northwestern United States. *J. Sed. Petrol.* 54: 86-97.

Pritchard, D.W. 1956. The dynamic structure of a coastal plain estuary. *J. Mar. Res.* 15: 33-42.

Sharples, J., J.H. Simpson and J.M. Brubaker. 1994. Observations and modeling of periodic stratification in the upper York River estuary, Virginia. *Est. Coast. Shelf Sci.* 38: 301-312.

Signell, R. and W.R. Geyer. 1990. Numerical simulation of tidal dispersion around a coastal headland. In: R.T. Cheng (ed.), *Coastal and Estuarine Studies 38: Residual currents and long-term transport*, pp. 210-222, Springer-Verlag, New York.

Simpson, J.E. 1982. Gravity currents in the laboratory, atmosphere, and ocean. Ann. Rev. Fluid Mech. 14: 213-234.

Simpson, J.E. 1987. *Gravity Currents in the Environment and the Laboratory*. Cambridge University Press, 244 pp.

Thomson, R.E. and K.Y. Chow. 1980. Butterworth and Lanczos-window cosine digital filters: with application to data processing on the Univac 1006 computer. *Pac. Mar. Sci. Rep.* 80-9, Inst. of Ocean Sci., Patricia Bay, B.C., Canada, 60 pp.

Walters, R.A. 1982. Low-frequency variations in sea level and currents in south San Francisco Bay. *J. Phys. Oceanogr.* 2: 658-668.

Walters, R.A. and J.W. Gartner. 1985. Subtidal sea level and current variations in the northern reach of San Francisco Bay. *Est., Coast. and Shelf Sci.*, 21: 17-32.

Wang, D.P. and A.J. Elliot. 1978. Non tidal variability in the Chesapeake Bay and Potomac River: Evidence for non local forcing. *J. Phys. Oceanogr.* 8: 225-232.

Wang, D.P. 1979. Wind-driven circulation in Chesapeake Bay, Winter 1975. *J. Phys. Oceanogr.* 9: 564-572.

Weisberg, R.H. 1976. The nontidal flow in the Providence River of Narragansett Bay: a stochastic approach to estuarine circulation. *J. Phys. Oceanogr.* 6: 721-734.

Wiseman, W.J.Jr., E.M. Swenson and F.J. Kelly. 1990. Control of estuarine salinities by coastal ocean salinity. In: R.T. Cheng (ed.), *Coastal and Estuarine Studies 38: Residual currents and long-term transport*, pp. 184-193, Springer-Verlag, New York.

Wong, K.-C. 1994. On the nature of transverse variability in a coastal plain estuary. *J. Geophys. Res.* 99: 14,209-14,222.

Wong, K-C. and X. Lu. 1994. Low-frequency variability in Delaware's inland bays. *J. Geophys. Res.* 99(C6): 12,683-12,695.

Zimmerman, J.T.F. 1986. The tidal whirlpool: A review of horizontal dispersion by tidal and residual currents. *Neth. J. Sea Res.* 20: 133-154.

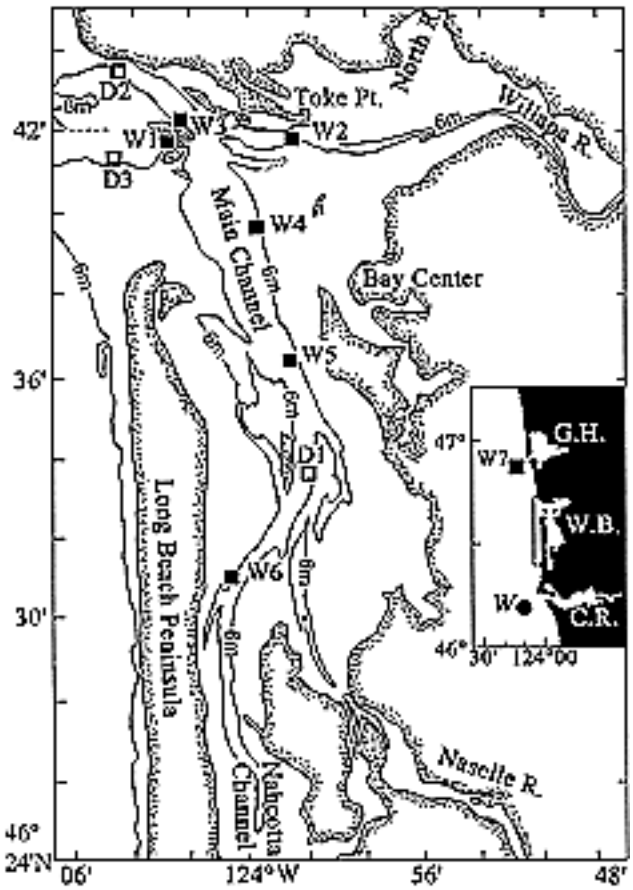

Figure1. Topography and setting of Willapa Bay with locations of moored current meters/temperature-conductivity sensors (squares), and with the larger scale setting shown on the inset map. Locations of the coastal estuaries are labeled GH (Grays Harbor), Willapa Bay (WB) and Columbia River (CR). Location of the wind measurement site is shown as a solid dot and denoted "*W*" on the inset map. Sites W1-W7 and D1 were occupied in summer 1995. Sites D2 and D3 were occupied in summer-early fall 1996. The prefix "W" is used to indicate single depth current meters (generally two per site at 8-15 m depths). The prefix "D" is used to indicate ADCP current profilers.

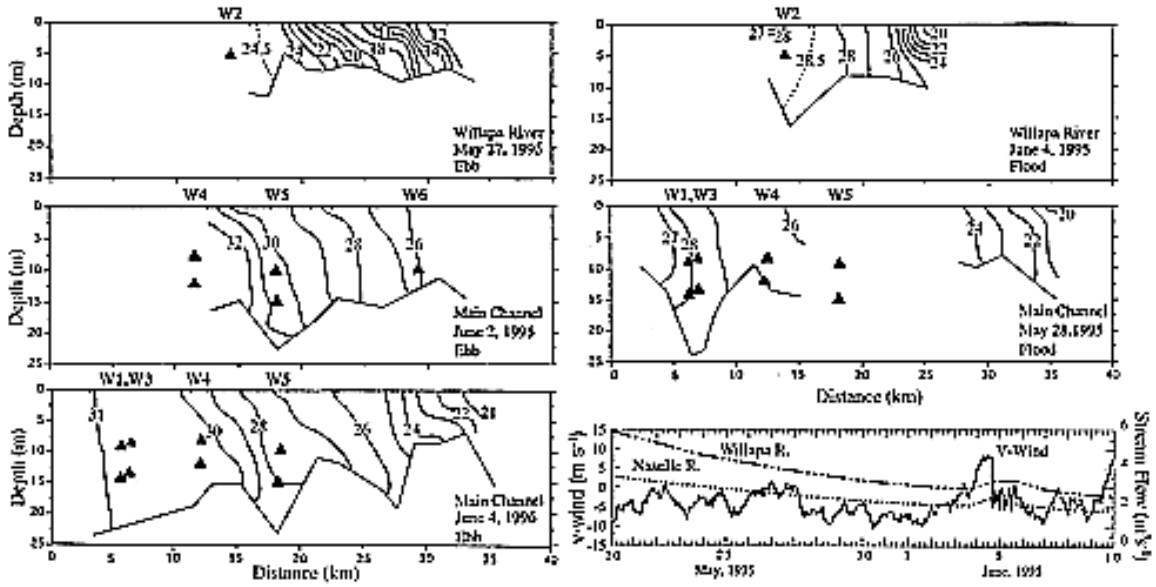

Figure 2. Contoured sections of salinity (2a), temperature (2b) and density (2c) along north-south (denoted "main channel") and east-west (denoted "Willapa River") branches of Willapa estuary. Distance is given in kilometers from the mouth of the estuary. Locations of moored sensors are shown as triangles on the salinity figure, with mooring labels given along the top of the figure. Environmental conditions at the time of the transect (gauged flow from the Naselle and Willapa Rivers and alongshore wind, shown positive northward) are presented as time series. Total flow is approximately equal to the sum of those two rivers multiplied by 5.32, a factor obtained using watershed area and gauge location.

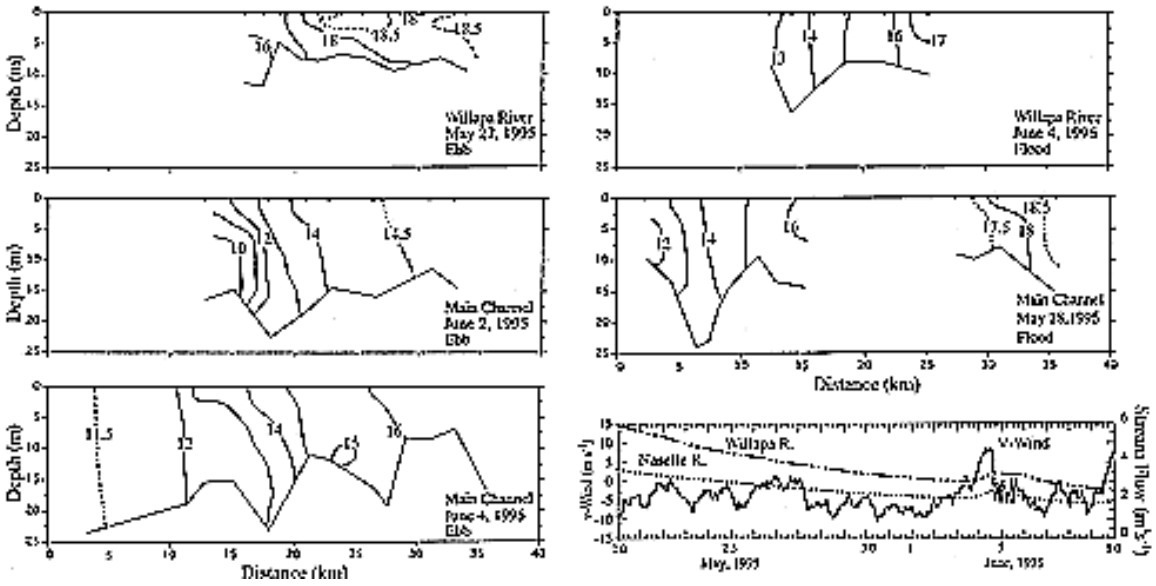
Willapa River
May 27, 1995
Ebb
Willapa River
June 4, 1995
Flood
Main Channel
June 2, 1995
Ebb
Main Channel
May 28,1995
Flood
Main Channel
June 4, 1995
Ebb
Depth (m)
Distance (km)
Willapa R.
Naselle R.
v-Wind
May, 1995
June, 1995

Figure 2b.

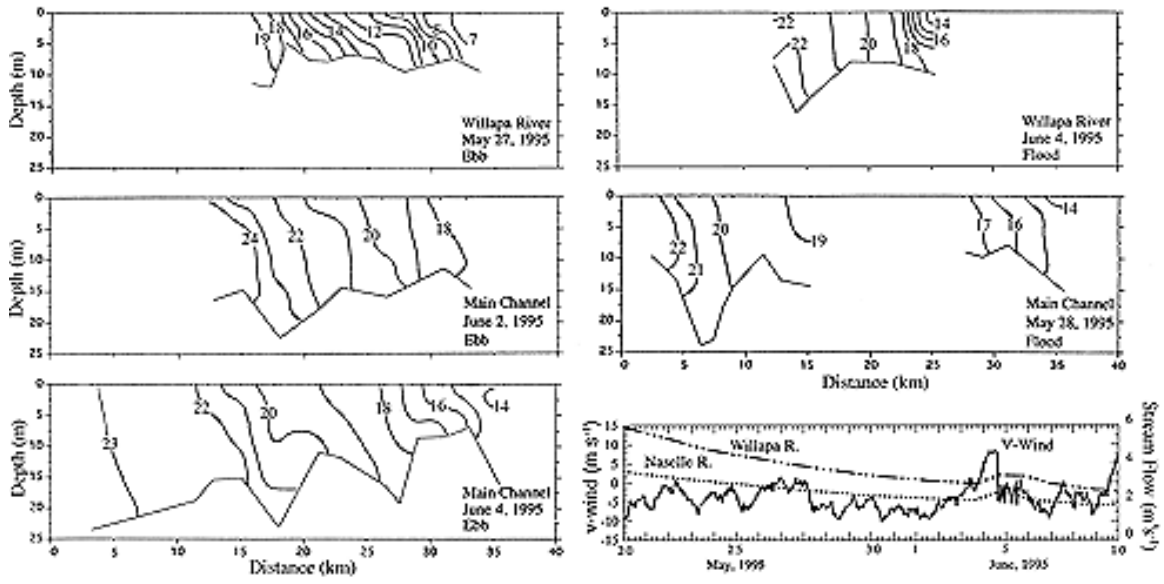
Depth (m)
Willapa River
May 27, 1995
Ebb
Willapa River
June 4, 1995
Flood
Main Channel
June 2, 1995
Ebb
Main Channel
May 28, 1995
Flood
Main Channel
June 4, 1995
Ebb
Distance (km)
v-wind (m s-1)
Willapa R.
Naselle R.
V-Wind
Stream flow (m3 s-1)
May, 1995
June, 1995

Figure 2c.

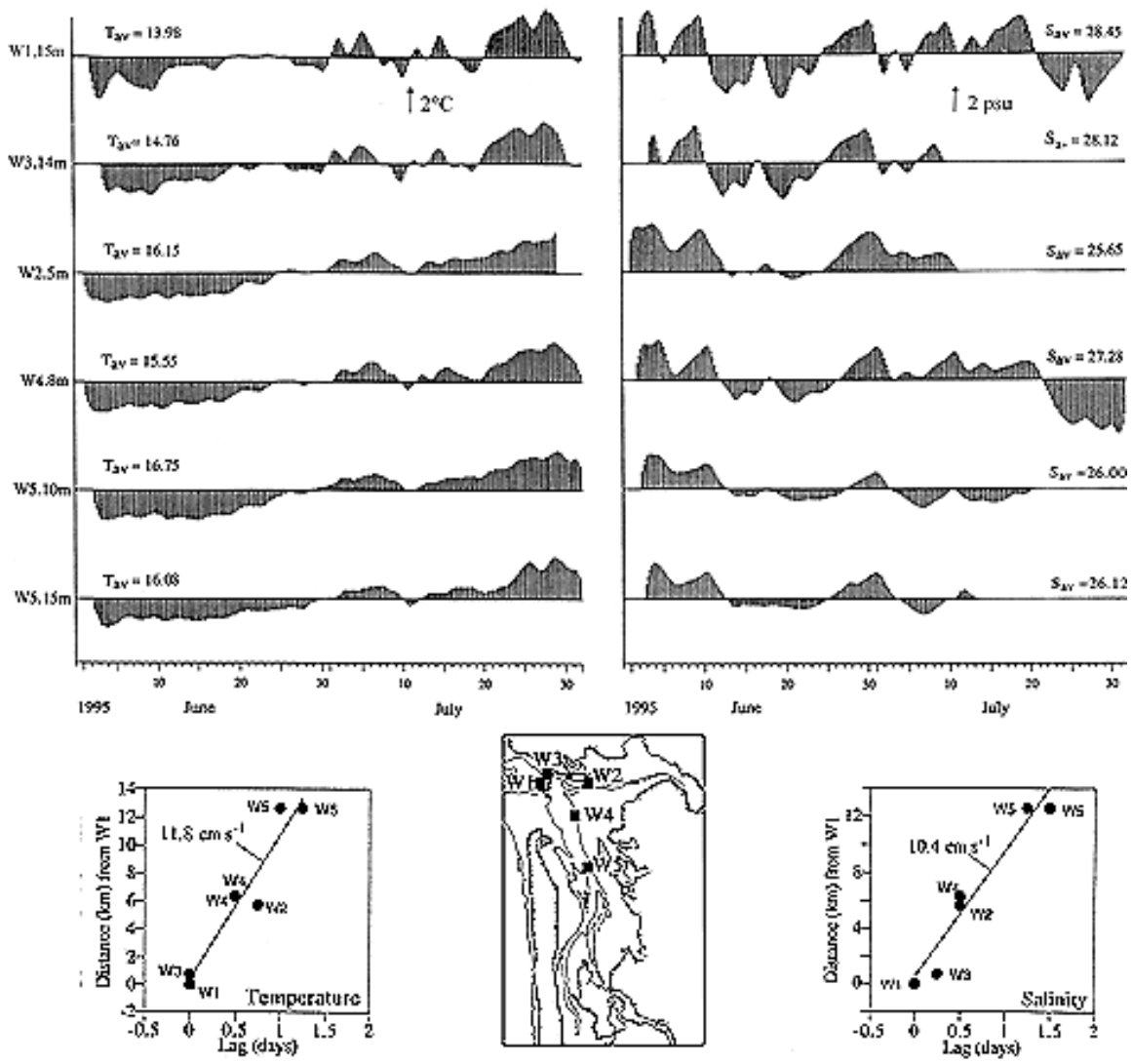

Figure 3. Residual time series of de-meaned temperature and salinity in Willapa Bay. Record means are given above each time series and denote the value at the axis. Note that data that exhibited biofouling was deleted from some salinity series so that the mean is not the mean of the portion of the record shown in the figure. Data are arranged from north to south (top to bottom panels) along the estuary, with W1 being closest to the ocean. Instrument depth in meters is given in the sensor label. Up-estuary delay of the temperature and salinity signals are shown in the bottom panels as the time lag for maximum correlation with the site near the mouth (W1). The slope of the regression line gives the apparent up-estuary propagation rate for each signal. All correlations are significant at the 90% level.

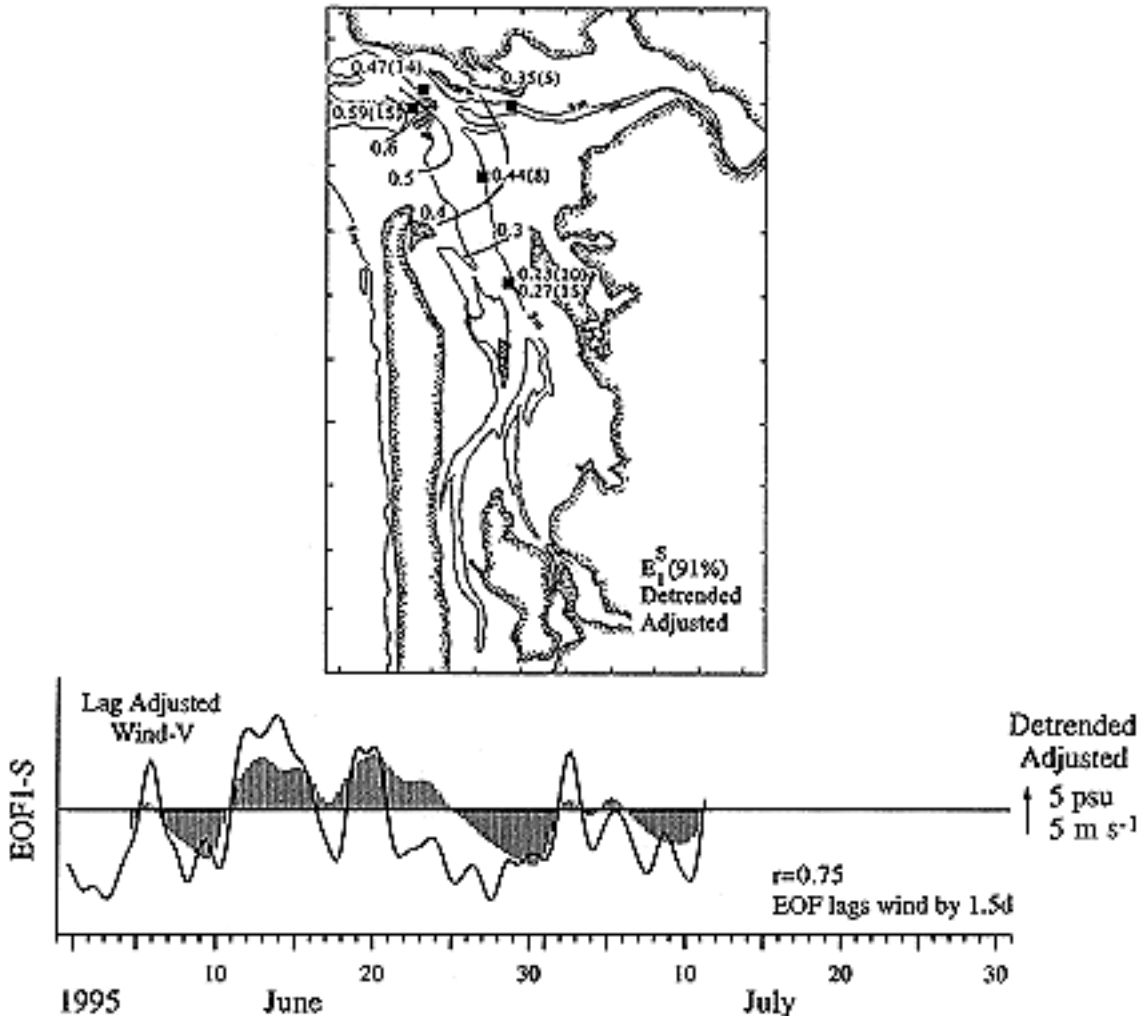

Figure 4. Amplitude (upper panel) and time series (lower panel) for salinity (4a) and temperature (4b) EOF analyses. Measurement depth in meters is given in brackets next to each value. Alongshore wind (positive northward) is shown as a line plot with the EOF amplitude time series. Wind has been advanced by the lag for maximum wind-EOF correlation. For temperature data, results are shown using both the unaltered data (upper time series and left panel) and the detrended, lag-adjusted data (lower time series and right panel). Salinity data are shown only for detrended, lag-adjusted data.

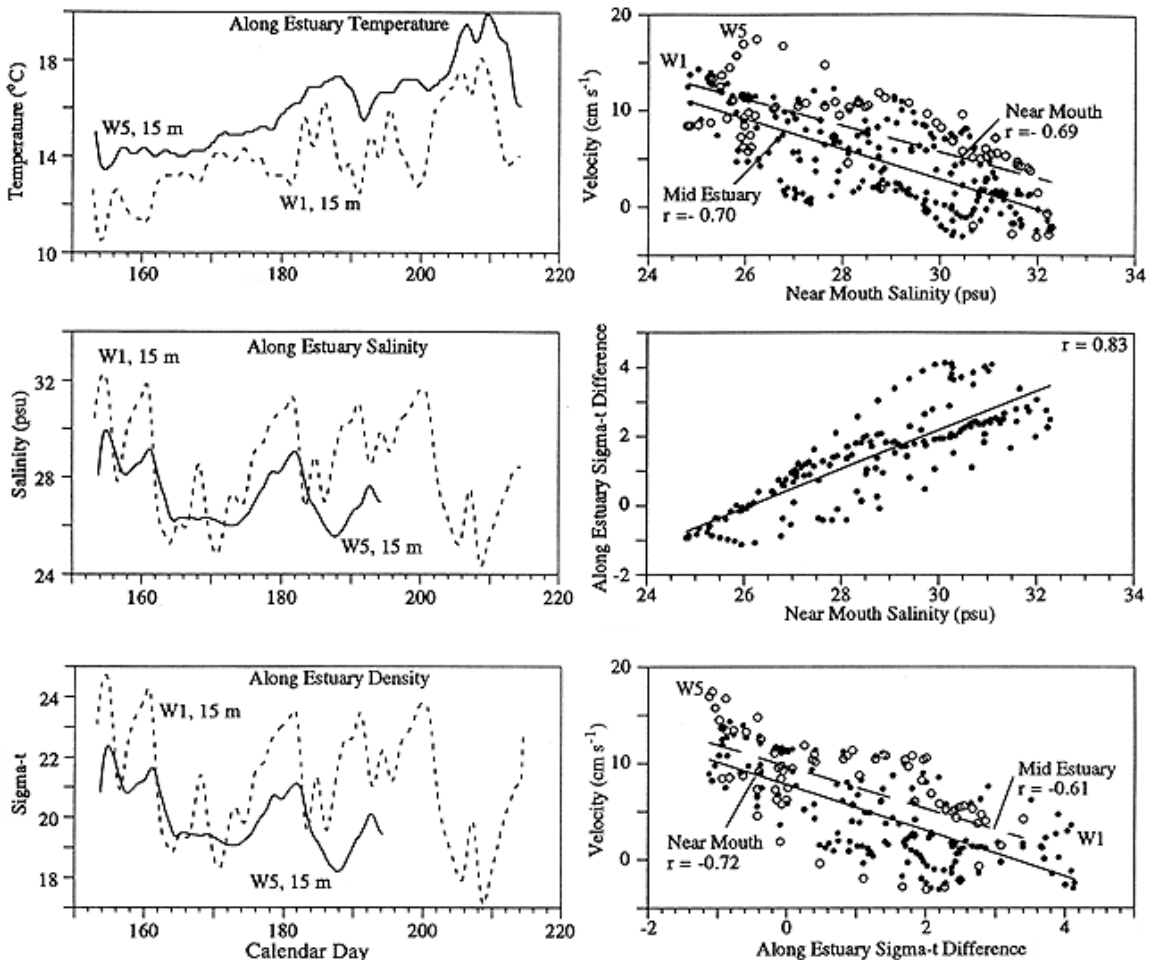

Figure 5. Left Panels. Along-estuary temperature, salinity and density time series. Right Panels. Velocity (top) and along-estuary sigma-t difference (middle) as a function of salinity near the mouth. Along-estuary velocity at two sites as a function of density difference between those sites (bottom). The slope of the regression is shown for each data pair.

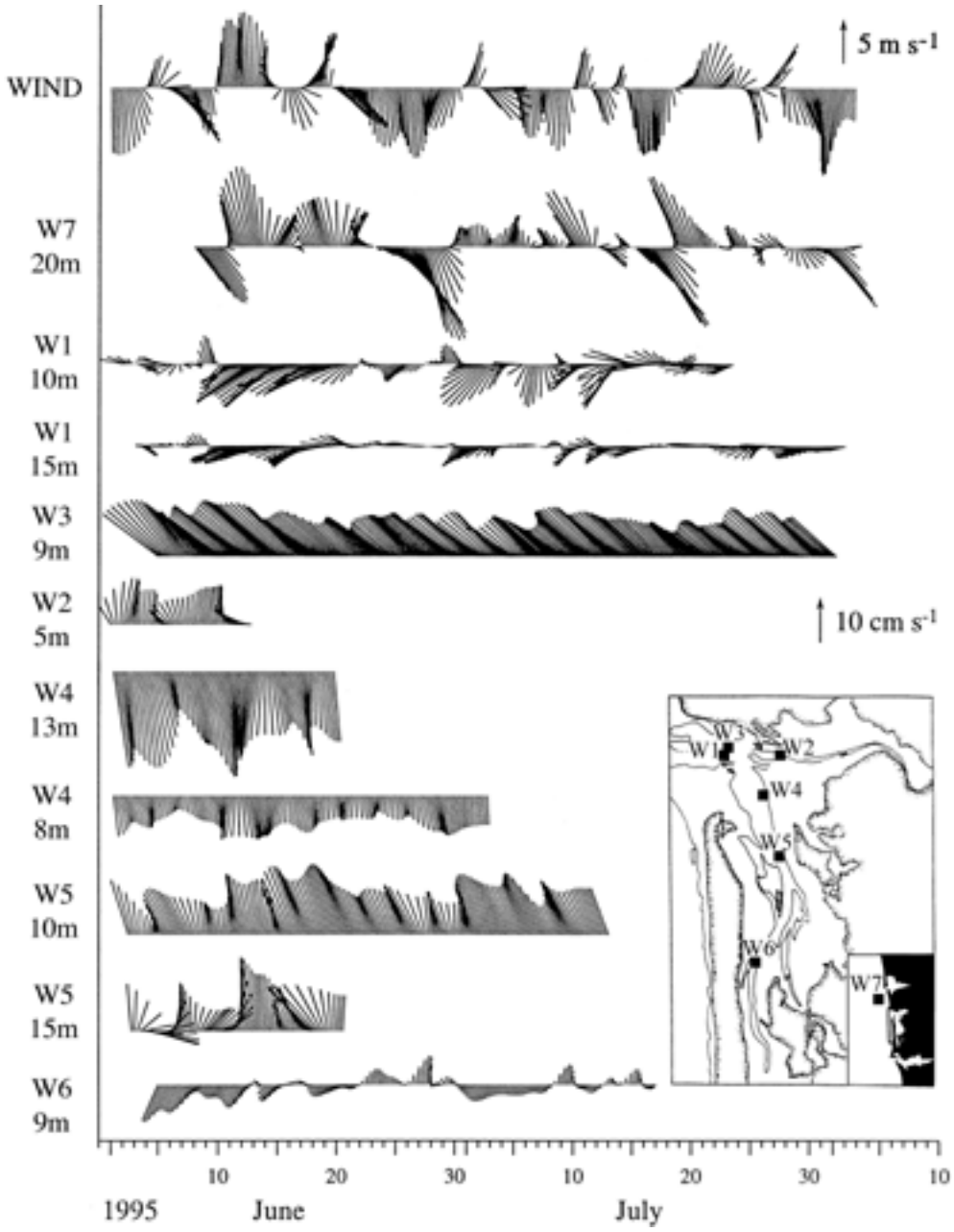

Figure 6. Residual time series of wind and vector velocity in a north-south reference frame (positive northward and eastward). Series are arranged with wind as the top panel, followed by coastal currents, and then estuary currents at locations from the mouth to the head. Measurement depth in meters is given in each site label.

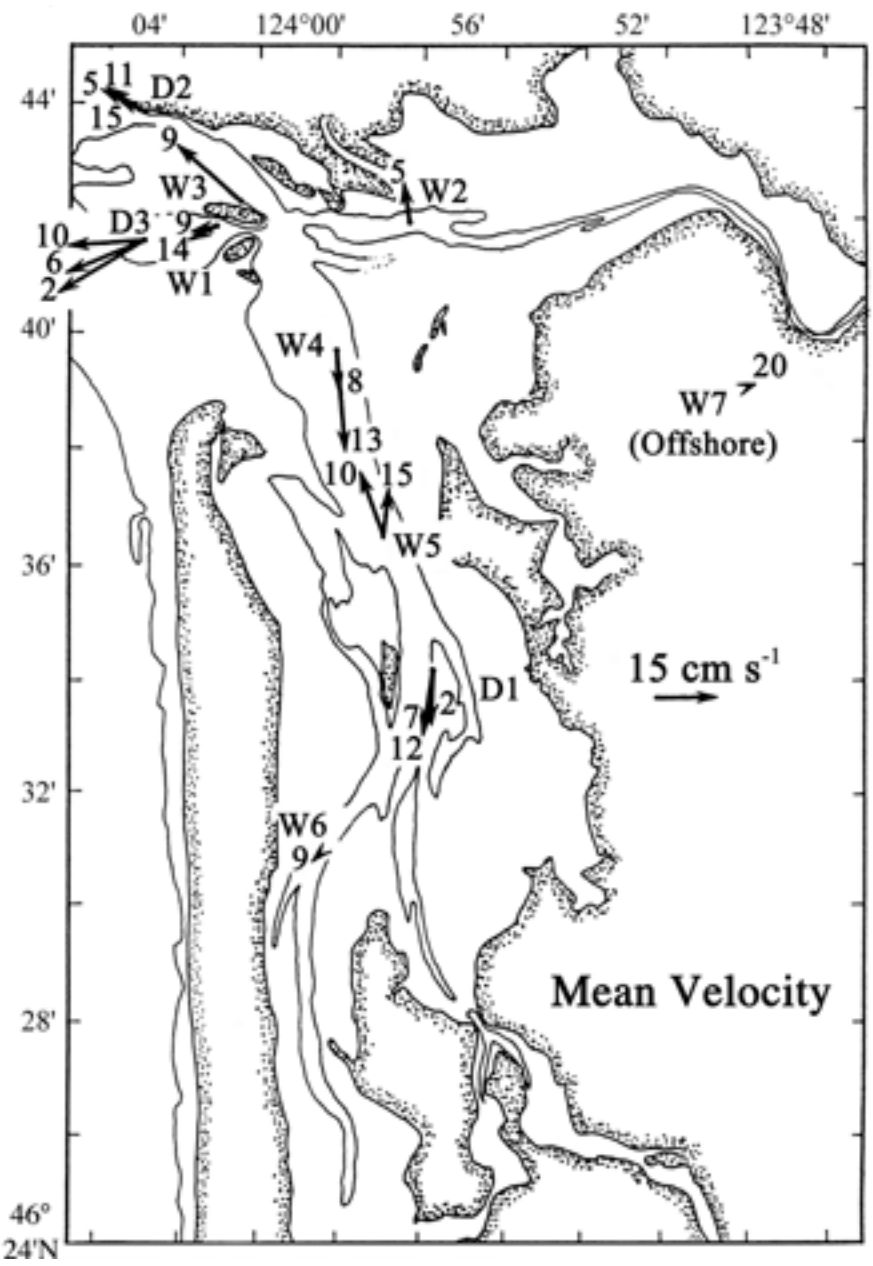

Figure 7. Mean wind and mean Eulerian currents on the shelf and in Willapa Bay. Means were calculated for available record lengths rather than for a common time period (see text). Sensor depth is given near the tip of each vector. The mean for the shelf site is shown on land in the upper right (W7).

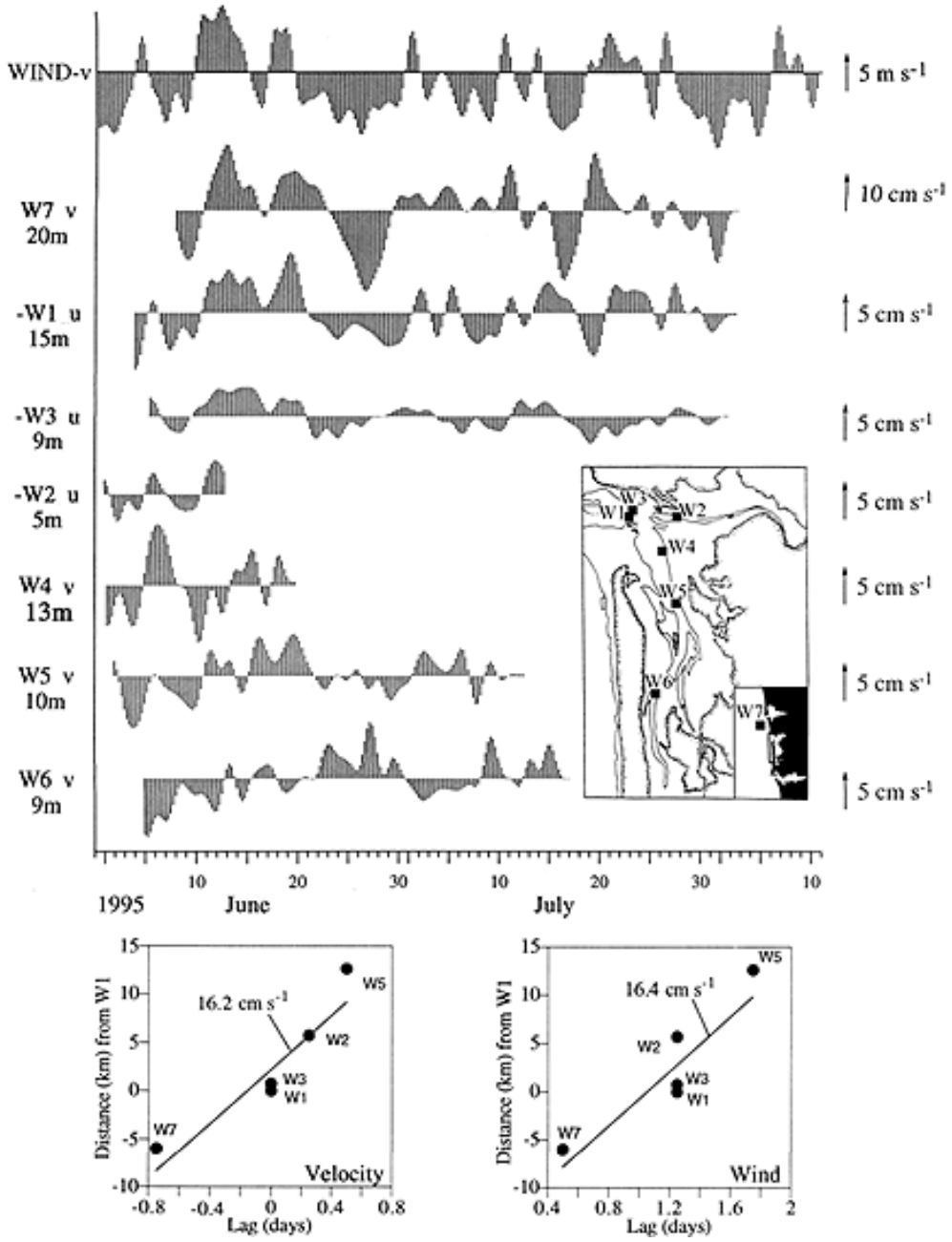

Figure 8. Dominant component of wind and Eulerian flow (positive northward or westward). Series are arranged with wind as the top panel, followed by coastal currents, and then estuary currents at locations from the mouth to the head in the bottom panel. Up-estuary delay of the velocity signal as well as the delay of velocity with respect to wind are shown in the bottom panels as the time lag for maximum correlation with the site near the mouth (W1) or with wind, respectively. The slope of the regression line gives the apparent up-estuary propagation rate for each signal. All correlations are significant at the 90% level.

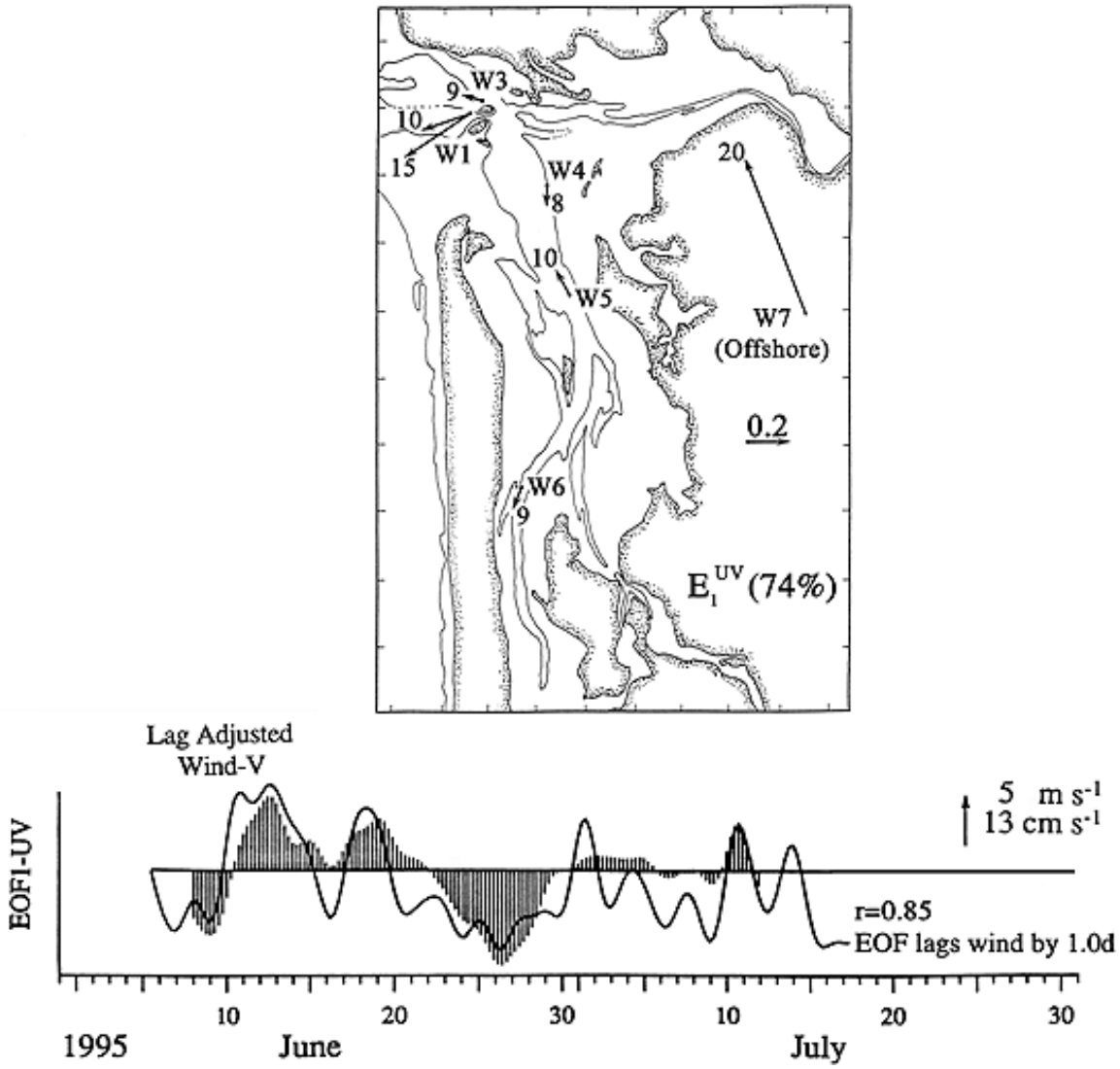

Figure 9. Amplitude (upper panel) and time series (lower panel) for velocity EOF analysis. Measurement depth in meters is given at the tip of each vector. The amplitude at the shelf site is shown on land in the upper right of the figure. Alongshore lag-adjusted wind (positive northward) is shown as a line plot with the EOF time series. Wind has been advanced by 1 d, the lag for maximum wind-EOF correlation.

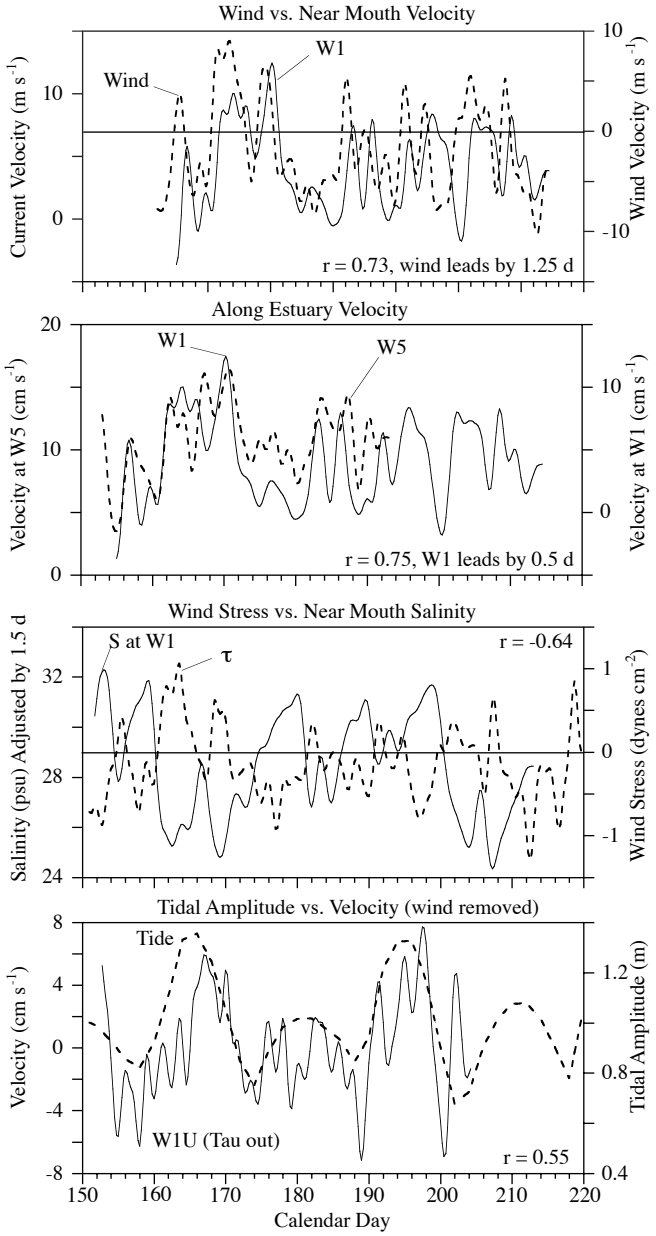

Figure 10. Top Panel. Alongshore wind stress and along-estuary currents near the estuary mouth (W1). Second Panel. Along-estuary currents near the mouth (W1) and halfway up the estuary (W5). Third Panel. Alongshore wind stress and salinity at the site nearest the estuary mouth, with salinity adjusted earlier in time by 1.5 d. Bottom Panel. Tidal amplitude and current at W1, where wind stress related variance has been removed from the velocity time series.

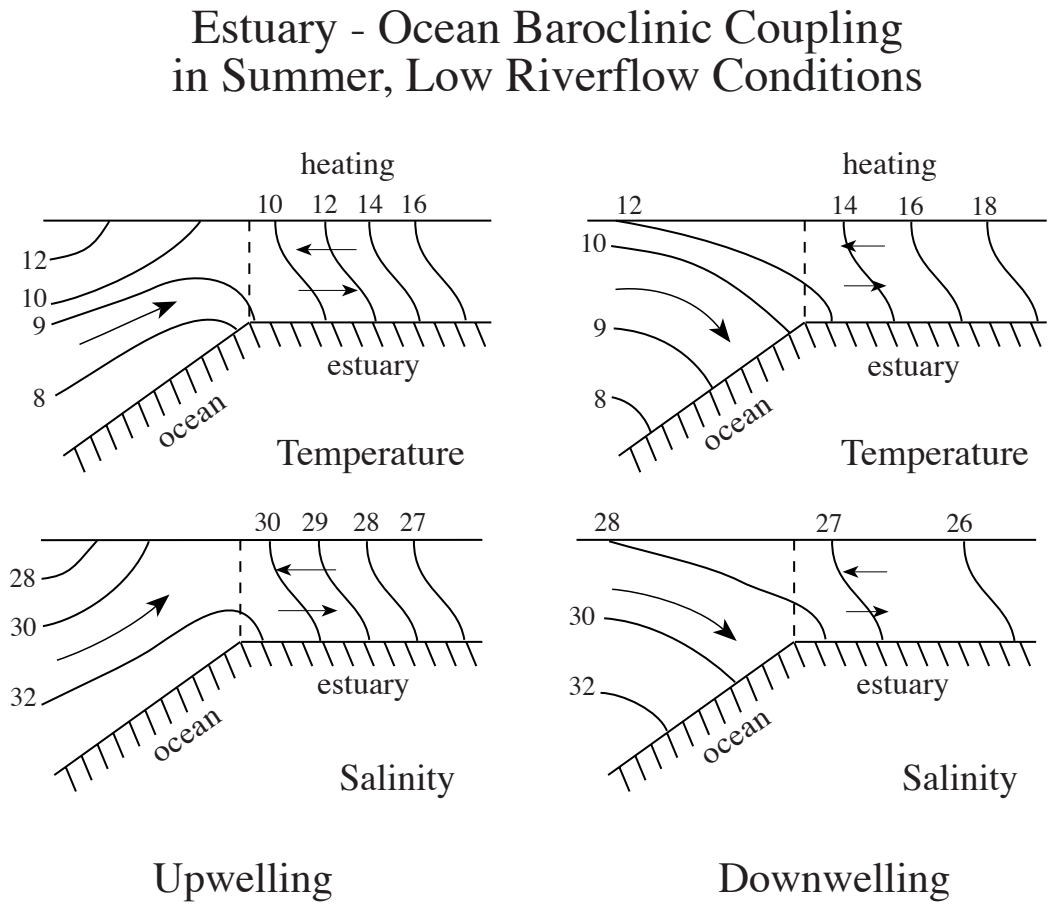

Figure 11. Schematic illustrating baroclinic coupling between the coastal ocean and a coastal plain estuary during upwelling and downwelling events for a low riverflow, summer period in an Eastern Boundary system.